

Solar radiation and atmospheric CO₂ predict young leaf production in a moist evergreen tropical forest: Insights from 23 years

Laura Lüthy^{1,2}, Colin A. Chapman^{3,4,5}, Patrick Lauer^{1,2,6}, Patrick Omeja⁷, Urs Kalbitzer^{1,2,8}

¹Department of Biology, University of Konstanz, Konstanz, Germany

²Max-Planck-Institute of Animal Behavior, Konstanz, Germany

³Biology Department, Vancouver Island University, Nanaimo, British Columbia, Canada

⁴Shaanxi Key Laboratory for Animal Conservation, Northwest University, Xi'an, China

⁵School of Life Sciences, University of KwaZulu-Natal, Pietermaritzburg, South Africa

⁶Max-Planck-Institute for Evolutionary Anthropology, Leipzig, Germany

⁷Makerere University Biological Field Station, Fort Portal, Uganda

⁸Centre for the Advanced Study of Collective Behaviour, University of Konstanz, Konstanz, Germany

Abstract

Climate change impacts ecosystems worldwide, affecting animal behaviour and survival both directly and indirectly through changes such as the availability of food. For animals reliant on leaves as a primary food source, understanding how climate change influences leaf production of trees is crucial, yet this is understudied, especially in moist evergreen tropical forests. We analyzed a 23-year dataset of young leaf phenology from a moist tropical forest in Kibale National Park, Uganda, to examine seasonal and long-term patterns of 12 key tree species consumed by folivorous primates. We described phenological patterns and explored relationships between young leaf production of different tree species and climate variables. We also assessed the suitability of the Enhanced Vegetation Index (EVI) as a proxy for young leaf production in moist evergreen tropical forests. Our results showed that tree species exhibited distinct phenological patterns, with most species producing young leaves during two seasonal peaks aligned with the rainy seasons. Rainfall, cloud cover, and maximum temperature were the most informative predictors of seasonal variation in young leaf production. However, solar radiation and atmospheric CO₂ were most informative regarding long-term trends. EVI was strongly correlated with young leaf production within years but less effective for capturing inter-annual trends. These findings highlight the complex relationship between climate and young leaf phenology in moist evergreen tropical forests, and helps us understand the changes in food availability for tropical folivores.

Significance

This study contributes to our understanding of seasonal and long-term variation in young leaf production recorded over 23 years in a moist evergreen tropical forest. Seasonally, trees showed a bimodal pattern of young leaf production aligned with the rainfall seasonality. With regard to long-term trends, solar radiation emerged as the primary driver of long-term phenological trends, with CO₂ fertilization contributing to productivity increases in some species. However, declines in young leaf production around 2001 and 2019 indicate the overriding influence of solar radiation. Despite these clear patterns at the community level, different tree species showed distinct patterns. These findings stress the importance of integrating species-specific and community-wide long-term data to better predict ecosystem responses to climate change and to guide conservation strategies for both plants and their consumers.

Highlights

- Young leaf production was highly variable over 23 years
- Young leaves are seasonal and showed maximum production during the two rain seasons
- Long-term patterns of young leaf production follow the solar cycle, but has also increased with increasing global atmospheric CO₂ levels
- The observed interspecific variation in seasonality and long-term trends may have important consequences for herbivores, and what climate change will mean for them
- EVI is a good proxy for young leaf availability in a moist evergreen forest, but not for long-term trends

Introduction

Climate change has transformed marine, terrestrial, and freshwater ecosystems, causing local species losses and even led to the first climate-driven extinctions (IPCC, 2022). The tropics, which contain the majority of Earth's biodiversity, are especially vulnerable (Barlow et al., 2018), and it has been estimated that an overwhelming majority of vertebrate species extinctions have been of species using the tropics (Barlow et al., 2018; *IUCN. IUCN Spatial Data.*, 2018). Tropical environments include some of the hottest places on the planet but have the lowest inter-annual temperature variability (Mahlstein et al., 2011; Williams et al., 2007). Because of climate change, the tropics will thus experience climatic conditions without present-day equivalents (Mahlstein et al., 2011). Because species in the tropics are usually not adapted to strong climatic variation, their potential to adjust to rising temperatures is uncertain (Khaliq et al., 2014).

Projected climate change in the tropics includes increased rainfall variability, higher temperatures, and more extreme weather events, such as intense storms, droughts, and wildfires (Brando et al., 2019; Malhi et al., 2014; Zelazowski et al., 2011), but how these factors impact animal populations is poorly understood. We know that climate change can impact animal populations by increasing their extinction risk and lowering survival (Ozgul et al., 2023; Paniw et al., 2019), as well as by influencing habitat use, and foraging behaviour and efficiency (Beever et al., 2017; du Plessis et al., 2012). Additionally, climatic factors, such as rainfall and temperature, affect animal activity, diet, and foraging strategies either directly or indirectly by altering variables such as food availability (McFarland et al., 2014; Zhang et al., 2023).

Many animals rely on plant-based resources, thus the impact of climate change on patterns of leaf production, flowering, and fruiting of trees (i.e., plant phenology) can influence the distribution, behaviour, and survival of animals (Van Schaik et al., 1993). Different animals specialize on different plant parts, linking their survival to fluctuations in plant part availability. For example, among primates some mainly feed on fruits, others on insects, and yet others on leaves (Hawes & Peres, 2014). Although leaves have often been viewed as an abundant resource for folivores in tropical forests, studies show that folivorous primates exhibit strong preferences for young leaves and only occasionally consume mature leaves, usually when young leaves are less available (Chapman & Chapman, 1999; Lauer et al., in press; Waterman & Kool, 1994). Additionally, ashy red colobus monkeys (*Ptilocolobus tephrosceles*) were shown to have a strong preference for young leaves from a select few species (Lauer et al., in press). Similarly, black-and-white colobus monkeys (*Colobus guereza*) have been shown to prefer young leaves and shift to more diverse diets as young leaf availability declines, which highlights their dependence on seasonal changes, and the need to better understand young leaf phenology (Matsuda et al., 2020). However, how projected climate change impacts tropical phenology, and especially the phenology of young leaves, remains limited due to the difficulty of detecting long-term phenological patterns and identifying the environmental drivers of these patterns (Sullivan et al., 2024).

Most tropical trees exhibit seasonal fluctuations in the availability of young leaves and fruits, especially in areas with marked rainfall seasonality (van Schaik & Pfannes, 2005; Wright & van Schaik, 1994). There is some consensus that tropical leaf phenology may be mainly limited by water and solar radiation, with solar radiation decreasing with cloud cover (Hastenrath, 1985; Wright & van Schaik, 1994). While water availability and solar radiation are widely regarded as key drivers of leaf phenology, the impact of these factors can vary, with leaf flushing often aligning with peaks in solar radiation when water is not a limiting factor (Barone, 1998; Chen et al., 2021; Janssen et al., 2021; Van Schaik et al., 1993; Wagner et al., 2017; Wright & van Schaik, 1994). Thus, long-term changes in rainfall and solar radiation may also affect long-term patterns of young leaf phenology.

Additionally, increasing levels of atmospheric CO₂ and rising temperatures may affect phenological patterns. In fact, there has been a global greening trend, measured by remote sensing, probably due to fertilization caused by rising CO₂ levels (Piao et al., 2019; Zhu et al., 2016). Elevated atmospheric CO₂ concentrations can accelerate photosynthesis while limiting leaf transpiration, thus improving water-use efficiency (Ainsworth & Rogers, 2007; Keenan et al., 2013). However, a decline of the carbon fertilization effect within recent years has been suggested (Wang et al., 2020). Similarly, while higher temperatures may accelerate photosynthesis, they can also raise vapor pressure deficits, potentially leading to declines in photosynthetic rates under extremely hot conditions (Lewis et al., 2004; Lloyd & Farquhar, 2008).

Large-scale climate phenomena, such as the El Niño Southern Oscillation (ENSO) can also be important drivers of tropical phenology (Chang-Yang et al., 2016; Chapman et al., 2018). ENSO influences inter-annual variability in rainfall and temperature across regions. While ENSO has been identified as a driver of fruiting in many tropical areas, another independent ocean circulation system, the Indian Ocean Dipole (IOD), may also be important for shaping climate variability in Eastern Africa (Marchant et al., 2007). Whereas ENSO patterns have been shown to drive the interannual variability in seasonal rainfall patterns and temperature anomalies in and around Central America (Campos, 2018; Timmermann et al., 2018), IOD patterns may similarly impact rainfall in East Africa (Marchant et al., 2007).

Given the limited understanding of leaf phenology in moist tropical forests and its relationship to climate and food availability for folivores, this study aims to describe young leaf availability patterns and the climatic factors influencing these patterns in Kibale National Park, Uganda (hereafter Kibale). We focus on tree species consumed by the endangered ashy red colobus monkey, an important folivorous species in Kibale, whose diet primarily consists of young leaves (Chapman & Chapman, 2002; Lauer et al., in press). Red colobus monkeys are considered early indicators of a larger faunal decline, with the largest and most viable population of ashy red colobus living in Kibale, a moist tropical forest, which serves as a conservation refuge for many species (Linder et al., 2021). Thus, the young leaf phenology patterns of tree species consumed by red colobus are highly relevant for the ecosystem in Kibale and likely other central African tropical forests.

Kibale's climate has already experienced significant changes, with maximum and minimum temperatures increasing by approximately 1°C from 1970 to 2020 (Chapman et al., 2021). Although current precipitation levels remain relatively stable, future projections suggest increases of 2.5-5.0% per degree of global warming, alongside further temperature rises (Graham et al., 2016).

In this study, we analyzed two decades of phenological data to describe the seasonal and long-term patterns of young leaf production and examine associations with climatic variables. Additionally, we assessed the Enhanced Vegetation Index (EVI), a satellite-based measure of canopy "greenness", as a scalable proxy for monitoring leaf phenology in moist-evergreen tropical forests, comparing it to our manually collected field data to explore its potential for broader applications in phenological monitoring.

Material & Methods

Study site

The data for this study was collected in Kibale National Park, a mid-altitude, moist-evergreen forest in western Uganda (0°13'–0°41'N and 30°19'–30°32'E) (Chapman et al., 2010; Chapman & Lambert, 2000). The field site is situated near the Makerere University Biological Field Station (MUBFS). Rainfall in this area is bimodal, with two wet seasons and annual average rainfall of 1646 mm (Chapman et al., 2021). The phenological data for this study was collected within the Forestry Compartment K30, a section of the forest that has never been harvested with exception of a few large stems that have been removed by pitsawyers prior to 1970 (Chapman et al., 2010; Chapman & Chapman, 1997). This area has previously been described as a relatively undisturbed mature forest (Skorupa, 1988; Struhsaker, 1975) or as a relatively undisturbed old forest (Struhsaker, 1997).

Phenology Data

Data on the phenology of young leaves were collected approximately every 4 weeks between February 1999 and December 2021 by the long-term field assistant of the project. Each sampling was assigned to a specific month. Data collection was only paused from April to June 2020 due to the Covid-19 pandemic. For each record, the tree crown of each phenology tree was visually examined from the ground and given a young leaf score (YL) from 0-6, with zero representing no young leaves, and 6 the maximum amount of young leaves. All observations were conducted by the same long-term field assistant since 1999. For our analysis, we included data from 12 tree species that represent the most consumed species by folivorous red colobus monkeys in the area. These species make up ~50% of their diet, each species contributing at least 1% (Lauer et al., in press). In total, we included 30103 observations of these 12 species in our analysis, with an average number of 10.2 individual trees per species and month (range = 1-26), and between 84 and 248 trees every month.

Abiotic variables

We used rainfall data collected at the field site using a circular rain gauge, summarized per month in mm. Since temperature data collected at the same weather station was impacted by relocations and changes of thermometers (described in Chapman et al., 2021), we used the CRU TS v. 4.07 dataset to obtain monthly maximum temperature (hereafter T_{\max}) and minimum temperature (hereafter T_{\min}) values (https://crudata.uea.ac.uk/cru/data/hrg/cru_ts_4.07/) (Harris et al., 2020). Monthly downward surface shortwave radiation data (hereafter solar radiation, in W/m^2) was derived from the TerraClimate database accessed through Google Earth Engine (Abatzoglou et al., 2018; Gorelick et al., 2017). Monthly cloud fraction data represents the percentage of cloudy pixels in a grid cell, which we derived from the satellite-based data record CLARA-A3, created by the EUMETSAT's Satellite Application Facility on Climate Monitoring (CM SAF) (Karlsson et al., 2023). Additionally, we included atmospheric CO_2 (ppm) from globally averaged marine surface monthly mean data (Lan et al., 2024).

We also considered the intensity of the El Niño Southern Oscillation (ENSO) and Indian Ocean Dipole (IOD). For ENSO, we included the monthly timeseries of the Multivariable ENSO Index Version 2 (MEI.v2, <https://psl.noaa.gov/enso/mei/>). The MEI.v2 is calculated based on the five different variables sea level pressure, sea surface temperature, zonal and meridional components of the surface wind, and outgoing longwave radiation (Kobayashi et al., 2015). The IOD is represented by the anomalous sea surface temperature gradient between the western equatorial Indian Ocean and southeastern equatorial Indian Ocean, the Dipole Mode Index (DMI; Saji & Yamagata, 2003). Both the MEI.v2 and DMI were downloaded from the NOAA Physical Sciences Laboratory (<https://psl.noaa.gov/data/timeseries/month/DS/DMI/>, <https://psl.noaa.gov/enso/mei/>).

Plant productivity may not only be impacted by climatic conditions measured at the time of plant productivity assessment but also by the conditions in the months before. To investigate such lagged effects of rainfall, solar radiation, T_{max} , T_{min} , cloud cover and atmospheric CO_2 on young leaf phenology, we included additional time-lagged variables for 1 month (1m), 3 months (3m), and 6 months (6m) before each YL data point. For rainfall, we used the amount of rainfall in the previous month, and the sum of the amount of the previous 3 and 6 months. For all other variables, we included the values from the previous month, as well as the average of the previous 3 and previous 6 months. In total, we considered 26 climatic variables, including the lagged effects.

Enhanced Vegetation Index (EVI)

To assess whether local YL patterns in moist evergreen forests can be assessed using remote sensing data, we used the Enhanced Vegetation Index (EVI). The EVI is an indicator of vegetation greenness and correlates with ground measurements of gross photosynthesis (Gao et al., 2000; Huete et al., 2006), and has previously been shown to be sensitive to young leaves (Gonçalves et al., 2020; Liu et al., 2024). It is also viewed as an improved vegetation index compared to the Normalized Vegetation Index (NDVI), since it additionally includes a blue band and aerosol resistance coefficients for its calculation (Huete et al., 2000). In part, this solves the limitation of the NDVI index regarding saturation and sensitivity to atmospheric aerosols (Huete et al., 2002; Xiao et al., 2003).

We extracted EVI values for our study area for the period between February 2000 and December 2021 using the Terra-MODIS 250m 16-day V6.1 product MOD13Q1 and the Aqua-MODIS 250m 16-day V6.1 product MY13Q1 V6.1 (Didan, 2021a, 2021b) accessed via Google Earth Engine (Didan et al., 2015; Gorelick et al., 2017) and as detailed in the Supporting information (Method S1)

Statistical modelling

We calculated Bayesian Generalized Additive Mixed Models (GAMMs) to assess the temporal variability in climate variables and young leaves, as well as the relationships between climatic variables and young leaves. All analyses were conducted using the R statistical programming language version 4.3.2 (R Core Team, 2023) in combination with brms version 2.20.12 (Bürkner, 2017), which uses Stan via the CmdStanR package version 0.7.1 in the background (Gabry et al., 2024).

To describe the seasonal and long-term patterns for each climate variable, we constructed GAMMs with the climate variable as normally distributed response variable, and two different splines as predictor variables, one cyclic cubic spline with month of the year as predictor (hereafter seasonal spline, number of knots $k = 12$, one for each month) and one (non-cyclic) cubic spline with month since first observation as predictor (hereafter trend spline, number of knots $k = 22$, one for each year; Table 1). The seasonal spline represents the seasonal component, while the trend spline represents long-term trends. Together the seasonal spline, trend spline, and intercept result in the model predictions.

To describe the young leaf phenological pattern of the plant community (all 12 species together), we constructed a Hierarchical GAMM (HGAMM), and accounted for species-specific patterns (Pedersen et al., 2019). We used the young leaf scores (0-6) as outcome variables in a binomial model with six trials and added the ID of the individual trees (TreeID) as a grouping variable. These models had the same two global smooth terms, one seasonal and one trend spline, as the climate models. The community model also included two group-level smooth terms to account for interspecific differences (Table 1). These group-level smooth terms are the tensor products of the continuous smoothers for month of the year and months since first observation, respectively, and a smooth-by term for the grouping variable, in our case the species, using a factor-smoother interaction basis (“fs”; Pedersen et al., 2019). Hereby a copy of each set of basis functions is created for each species with the same flexibility, or “wiggleness” for all species as described by Pedersen et al. (2019) as “GS model”. Therefore, we

obtained estimates for global (i.e., community-level) seasonal and trend splines as well as species-specific splines from the same model. In other words, the global splines in this model accounted for inter-specific differences.

To determine the young leaf phenology patterns and their association with the climate variables for each species individually, we constructed multiple GAMMs with and without spline terms and climate variables as predictors (Table 1). As above, we used YL (0 - 6) as outcome variable in binomial GAMMs with six trials and added TreeID as a grouping variable. All climatic variables were centered at 0 and scaled to 1 SD before running the analysis. We constructed seven different types of models for each species: (1) An intercept-only model, (2) a model with the seasonal and trend spline, (3) a model only with the seasonal spline, (4) a model only with the trend spline, (5) models only with a single climate variable as predictor, (6) models with the seasonal spline and a single climate variable as predictor, and (7) models with the trend spline and single climate variable as predictors (Table 1). In each model, only a single climate variable was included at a time to avoid the inclusion of correlated climate variables in the models. By substituting either the seasonal spline or trend spline with a climate variable, we investigated the association between the climate variables and YL while accounting for none, the seasonal pattern, or the long-term patterns using the two splines. As a result, we ran 82 different models for each species. We did not perform this analysis for the community HGAMM because the community-level young leaf phenology is driven by the aggregated effects of individual species, making it redundant to model the same climate variables at the community level.

We compared these models using the Bayesian LOO estimate of the expected log pointwise predictive density (ELPD LOO) to find the most informative models (Vehtari et al., 2017). This is done by evaluating the log-likelihood at the posterior simulations of the parameter values, where a lower ELPD-LOO value indicates a more informative model. Next, we calculated the differences in ELPD-LOO values between the model with the lowest ELPD-LOO (the most informative model) and each of the other models. To estimate the difference in the expected predictive accuracy between the model with the lowest ELPD-LOO and each other model, we computed the standard error of the difference in ELPD-LOO values between models. These calculations were done using the brms package version 2.20.12 (Bürkner, 2017). For our analysis, we considered models where either the seasonal spline or trend spline was replaced by the climate variable that resulted in the smallest ELPD-LOO, indicating the strongest predictive performance. Models were considered equally informative if their ELPD-LOO was within two standard errors of the difference compared to the model with the lowest ELPD-LOO.

To analyse EVI, we first constructed a model with the same seasonal and trend spline terms used in the previous models. We then compared the relationship between monthly YL and EVI at three different levels: (1) observed data over the entire monthly time series, (2) seasonal spline means derived from the EVI model and the YL community HGAMM, and (3) trend spline means from the EVI and YL models. For each level, we evaluated the relationship using three approaches: (i) Pearson correlations to quantify the linear association, (ii) cross-correlation functions (CCF) to identify potential time lags, and (iii) Bayesian linear models to estimate the effect of YL (predictor) on EVI (response). Specifically, for the seasonal and trend spline levels, Bayesian models were fit using the posterior means of the respective smooth terms as the predictor and response variables.

Table 1 Simplified model formulas for climate variables (CV) and phenology GAMMs. Month = month of the year; MonthSinceStart = month since first observation. Seasonal spline = cyclic spline term, trend spline = cubic, non-cyclic spline term.

Model type	Model formula
Climate	CV ~ seasonal spline + trend spline

Young leaf phenology pattern (Community HGAMM)	$YL \sim \text{seasonal spline (Month)} + \text{seasonal spline (Month, Species)} + \text{trend spline (MonthSinceStart)} + \text{trend spline (MonthSinceStart, Species)} + (1 TreeID)$
Association between climate variables (CV) and young leaf phenology scores (YL) for model comparison (for each species separately)	$YL \sim 1 + (1 TreeID)$
	$YL \sim \text{seasonal spline} + \text{trend spline} + (1 TreeID)$
	$YL \sim \text{seasonal spline} + (1 TreeID)$
	$YL \sim \text{trend spline} + (1 TreeID)$
	$YL \sim CV + (1 TreeID)$
	$YL \sim \text{seasonal spline} + CV + (1 TreeID)$
	$YL \sim \text{trend spline} + CV + (1 TreeID)$

Ethics

The research described here was approved by the Uganda Wildlife Authority (UWA), Makerere University, and the Uganda National Council for Science and Technology (UNCST).

Results

Patterns of climatic variables

The rainfall model detected a bimodal seasonal pattern (Fig. 1a), with a smaller peak in April (164 mm; small rain season) and a larger peak in October (253 mm; large rain season), and rainfall minima in February (56 mm) and July (75 mm). As expected, the fraction of cloud cover followed a similar pattern (Fig. 1b), peaking in April (83 %) and October (85 %), and lows in January (65 %) and June (67 %). Maximum and minimum temperature only showed single main peaks, T_{max} in February (29.0 °C, Fig. 1c), and T_{min} later in April (17.0°C, Fig. 1d). The lowest T_{max} (27.0 °C) and T_{min} (15.8 °C) both occurred in July between the two rain seasons. Atmospheric CO₂ shows slight seasonality (Fig. 1e), with one peak in April (390.5 ppm) and a low in August (385.8 ppm). In contrast to this, solar radiation had several peaks per year (Fig. 1f), namely in February (2039 W/m²), May (1987 W/m²) and September (1940 W/m²), and was at its lowest in July (1798 W/m²). MEI values (indicating ENSO patterns, Fig. 1g) and DMI values (indicating IOD patterns, Fig. 1h) showed very little seasonality.

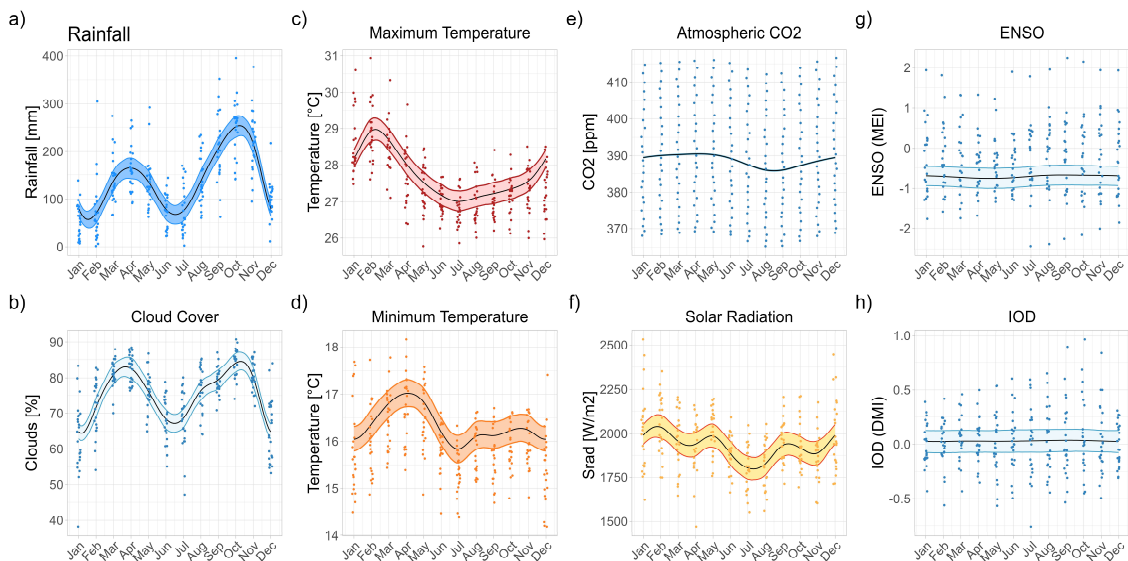


Figure 1 Seasonal splines of the climate models for (a) rainfall, (b) fractinal cloud cover, (c) T_{max} , (d) T_{min} , (e) atmospheric CO_2 , (f) solar radiation, (g) ENSO, and (h) IOD. Shaded areas represent the 95% credible interval of the estimated mean. Jittered points show the observed data.

Over the 23-year study period (1999–2021), the average yearly rainfall remained relatively stable, as indicated by the trend spline of the rainfall model (1999: 66.4 mm; 2021: 64.8 mm, Fig. 2a). In contrast, cloud cover showed a slight decrease (1999: 68.7%; 2021: 65.9%, Fig. 2b). Both average yearly T_{max} (1999: 27.3°C; 2021: 27.3°C, Fig. 2c) and T_{min} (1999: 15.4°C; 2021: 15.6°C, Fig. 2d) remained relatively stable over the study period, with a warmer period between 2000 and 2010. Global atmospheric CO_2 has been steadily increasing from 367.4 ppm in 1999 to 414.1 ppm in 2021 (Fig. 2e). The solar radiation trend spline exhibited more pronounced variability, with a decline from January 1999 to a low in April 2004 (1734 W/m², Fig. 2f), followed by an increase to a maximum in January 2017 (1970 W/m²), and another decline through the end of the study period. The trend spline of the MEI shows major ENSO events in 2010 and 2016 (Fig. 2g), as well as some smaller anomalies, while the DMI (IOD) exhibits much less variability, with peaks around 2007 and 2019 (Fig. 2h).

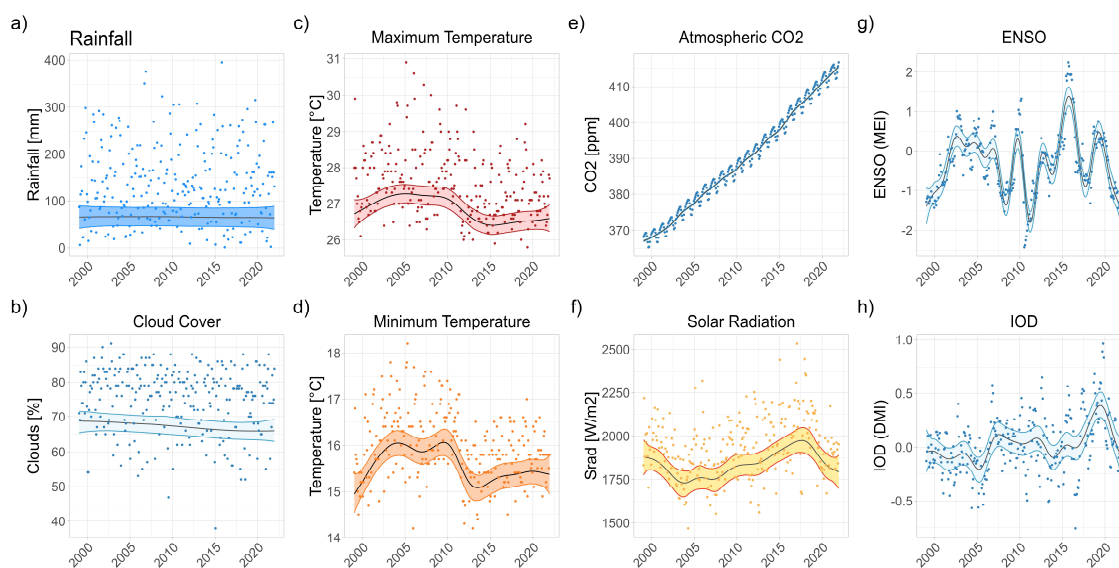


Figure 2 Trend splines of the climate models for (a) rainfall, (b) cloud cover, (c) T_{max} , (d) T_{min} , (e) atmospheric CO_2 , (f) solar radiation, (g) ENSO, and (h) IOD. Shaded areas represent the 95% credible interval of the estimated mean. Jittered points show the observed data.

Patterns of young leaf availability

Community-wide young leaf scores (all 12 species together) displayed a bimodal pattern with clear peaks in April and October (Fig. 3, Fig. S2). This bimodal pattern was also present in multiple species in the individual-species models (Fig. 3; Table S1), with variations in the relative magnitude of peaks. Two species (*Celtis gomphophylla*, *Albizia grandibracteata*) exhibited a larger peak in April and a smaller peak in October, while five species (*Millettia dura*, *Dombeya kirkii*, *Celtis africana*, *Macaranga schweinfurthii*, *Vepris nobilis*) showed approximately equally sized peaks in April and October, though species varied in magnitude. Three additional species (*Funtumia africana*, *Prunus africana*, *Parinari excelsa*) displayed weak seasonality, with peaks shifted to February/March and September/October. Another species (*Trilepisium madagascariense*) showed only very weak seasonality, and one species (*Strombosia scheffleri*) showed no seasonal pattern.

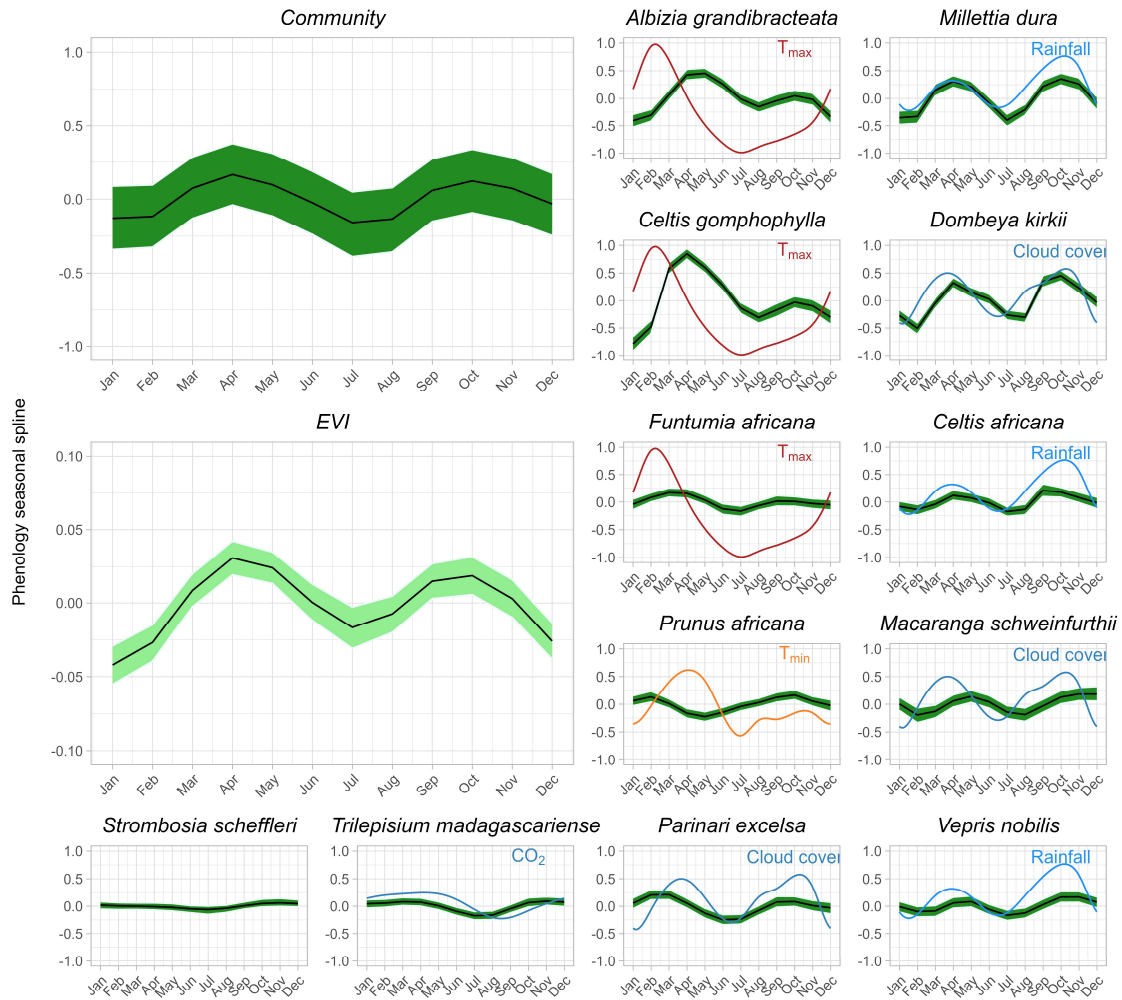


Figure 3 The seasonal splines from the community HGAMM and species-specific models for young leaf phenology scores and from the EVI model including the seasonal and trend spline. Shaded areas represent the 95% credible interval of the estimated mean, with the y-axis displaying the values of the trend spline estimates. Species are organized by phenological pattern. The most informative climate variable for each species is presented in the respective species plot (see Figure 1 for details on climate variables).

The HGAMM revealed significant long-term variability in young leaf production of the community over the 23 years of this study (Fig. 4, Fig. S2). Young leaf production initially peaked in 2001, followed by a decline and a period of low productivity from 2003 to 2006. This was succeeded by a steady increase, peaking around 2017, and a subsequent decline until the study's conclusion in 2022. Trends varied across species (Fig. 4, Table S2). Five species (*Vepris nobilis*, *Parinari excelsa*, *Dombeya kirkii*, *Strombosia scheffleri*, *Celtis africana*) exhibited an overall increase in young leaf production with an initial decline, a low around 2004-2006, followed by an increase to a peak around 2018/19, and then a gradual decrease. Another five species (*Funtumia africana*, *Albizia grandibracteata*, *Trilepisium madagascariense*, *Prunus africana*, *Millettia dura*) displayed a similar pattern but with smaller overall increases, starting with higher production, a low around 2006-2009, a peak in 2018/19, and then declined through 2022. Two species showed no such long-term increases: *Macaranga schweinfurthii*, which was only monitored until 2018 due to tree mortality, and *Celtis gomphophylla*, which exhibited high inter-annual variability rather than clear trends.



Figure 4 The trend splines from the community HGAMM and species-specific models for young leaf phenology scores and from the EVI model including the seasonal and trend spline. Shaded areas represent the 95% credible interval of the estimated mean, with the y-axis displaying the values of the trend spline estimates. Species are organized by phenological pattern. The trend splines for the two most predictive climate variables, solar radiation (red) and CO₂ (blue), are included in each plot (see Figure 1 for details on climate variables). For *Macaranga schweinfurthii* data was only available for part of the study period.

Association between climatic variables and young leaf phenology

When examining which climate variables were most closely linked to seasonal young leaf production, models with the lowest ELPD LOO often included different climate predictors, frequently with varying time lags across species (Table S1, and SI, Species specific tables). The associations that we detected were dependent on the degree of seasonality of young leaf production, because with no or little seasonality, there was less likely a link to climate variables. In addition, for seasonal species, the detected associations were dependent on during which month of the year a species was most likely to produce young leaves. For species with strong seasonality and a larger peak during the first wet season (April/May) compared to the second wet season (Oct/Nov), models including maximum temperature instead of the seasonal spline as predictor had the lowest ELPD LOO values. Here, higher T_{max} predicted increased young leaf production (Table S1). Similarly, in species that had equally high seasonal peaks during both rain seasons, the peak in young leaf production followed the peaks of rainfall and cloud cover. In contrast, species with weak seasonality and peaks preceding the rainy seasons showed no consistent association pattern with climate variables.

When examining long-term trends, models where trend splines were replaced with climatic variables revealed distinct patterns across species. Species that exhibited stronger increases in young leaf production over the study period were best predicted by atmospheric CO₂ (Table S2; *Vepris nobilis*, *Parinari excelsa*, *Dombeya kirkii*, *Strombosia schaffleri*, *Celtis africana*). Species with an initial peak in 2001, followed by a period of lower young leaf production, a subsequent increase until 2018/19, and a decline toward the end of the study period with a smaller overall increase aligned closely with models using the mean solar radiation from the previous six months as a predictor (Table S2; *Funtumia africana*, *Albizia grandibracteata*, *Trilepisium madagascariense*, *Prunus africana*, *Millettia dura*). In these cases, higher solar radiation in the previous six months was associated with increased young leaf production. This pattern corresponds to the overall trajectory of solar radiation, which decreased at the beginning of the study, peaked around 2017, and subsequently declined. For the species with the highest intra-annual variability, *Celtis gomphophylla*, and *Macaranga schweinfuthii*, which showed tree mortality, the long-term trend was also highly variable. No clear predictor emerged for these species; however, cloud cover from the previous month and solar radiation from the previous month were identified as the best predictors respectively.

EVI pattern and link to young leaf phenology

The EVI pattern generally corresponds to the pattern of the local young leaf phenology, with clear seasonal peaks in April and October (Fig. 3), and an overall increase in greenness over the years (Fig. 4). However, the trend spline for EVI values shows less inter-annual variability.

The observed monthly data of YL and EVI show a weak correlation ($r = 0.18$), with no time-lag identified by the CCF analysis (Fig. S1). The Bayesian linear model indicated a positive, though weak, relationship between YL and EVI (Estimate = 0.02, CI[0.01-0.04]). When comparing the seasonal splines of the YL and EVI seasonal spline trend spline models, we found a strong correlation ($r = 0.84$), again with no time-lag. The linear model showed a positive relationship (Estimate = 0.18, CI[0.1-0.27]). However, the trend splines showed a much weaker correlation ($r = 0.34$), and no clear time-lag pattern. The Bayesian linear model also suggested only a weak positive relationship between YL and EVI (0.01, CI[0.01, 0.01]). Taken together, this indicates a good correlation of YL and EVI for seasonal but not for long-term variation.

Discussion

In this study we characterized the climate patterns, as well as the seasonal and long-term young leaf phenology patterns in a moist tropical forest and related young leaf phenology to climate variables and EVI. At the community level, young leaf production was bimodally distributed, with peaks in April and October and low points in January and July. The peaks coincided with the rain seasons, whereas the low points coincided with dry season, also characterized by low cloudcover. The second low point in young leaf productivity in July furthermore coincided with minimal levels of solar radiation and temperature (Tmax and Tmin). Despite considerable interspecific variation, most species exhibited the lowest young leaf production in July. The climate variables most strongly associated with young leaf production during the year were rainfall, cloud cover, and maximum temperature, though the relationships varied by species.

Interestingly, the observed association of rainfall and cloud cover with seasonal young leaf production in this moist evergreen forest are in contrast with previous findings that found solar radiation to be the most important driver in the absence of water limitation. For example, Xiao et al. (2006) concluded that precipitation seasonality did not drive leaf phenology in tropical evergreen forests in South America, suggesting instead that solar radiation might play a more significant role. Similarly, earlier studies (Barone, 1998; Van Schaik et al., 1993; Wright & Van Schaik, 1994), observed young leaf peaks during periods of high solar radiation, provided that rainfall was not a limiting factor. However, Yang et al.,

2021 found that when peak solar radiation coincides with rainfall, leaf flushing tends to occur during the wet season. While leaf flushing in Kibale coincides with rainfall, solar radiation reaching the Earth's surface is reduced by cloud cover during the peak rain season, preventing solar radiation from peaking alongside rainfall.

We also observed considerable variation in young leaf phenology over the 23-year study period. Considering climatic factors, solar radiation and atmospheric CO₂ were the most important predictors of long-term changes in young leaf production. Most species exhibited a pattern of increases and decreases in long-term phenology, which closely followed the long-term solar radiation pattern associated with solar cycles. For species that showed an additional, stronger overall increase in production, atmospheric CO₂ presented as the best predictor. Even though CO₂ fertilization has decreased in recent years (Wang et al., 2020), our data still suggests a greening trend for multiple species, as is happening in most parts of the world (Piao et al., 2019). However, declines in production at the beginning of the study (~2001) and near the end (~2019) suggest that solar radiation is the more dominant driver of long-term young leaf phenology.

One crucial question is whether the observed long-term changes in young leaf phenology impacts the abundance and behaviour of red colobus in Kibale. While the number of red colobus groups declined between the 1970s and 1990s (likely due to logging in surrounding areas), their numbers have stabilized more recently (Chapman et al., 2023). This stability may reflect dietary flexibility, as red colobus monkeys may shift to alternative species when preferred ones are less available. However, the long-term pattern of young leaf production is in part reflected in the observed group size of red colobus in the same area (Chapman et al., 2023), with group sizes being significantly larger during periods of higher young leaf production, and becoming smaller when production is lower: according to Chapman et al. (2023), average group size from 1996-1998 was 30, increasing in 2010-2011 to 45, and in 2017-2018 to 75, and decreasing in 2022-2023 to 50. At the same time, we show here that young leaf phenology scores were increasing from 2006 to 2018, followed by a decrease until the end of the study. This suggests that red colobus showed a behavioural reaction to the changed food availability.

The differential responses of tree species to climate change complicate predictions of its impacts on herbivores, as community-wide evaluations risk overlooking species-specific dynamics that influence the availability of food for particular animal species. Our findings of interspecific differences in young leaf phenology patterns highlight that focusing solely on community-level phenology may not accurately reflect food availability for herbivores, such as red colobus monkeys, which exhibit strong dietary preferences (Lauer et al., in press). As plant species react differently to climate change, herbivores may need to adapt their feeding behaviour, potentially triggering cascading effects on their populations.

EVI proved to be a reliable predictor of within-year young leaf productivity, capturing seasonal fluctuations well. This also aligns with previous studies on young leaf phenology and EVI (Gonçalves et al., 2020; Liu et al., 2024). However, EVI showed limitations in capturing long-term trends. While EVI detected a general long-term increase in productivity, it failed to accurately reflect the recent declines indicated by our data collected on the ground. Additionally, relying solely on remote sensing data like EVI for phenology assessments risks masking species-specific phenological patterns, which are critical for understanding ecosystem dynamics and predicting the impacts on consumers.

Conclusion

Our study highlights the considerable seasonal and long-term variation in young leaf phenology patterns within a moist evergreen tropical forest. While the community-level trends reveal overarching seasonal and long-term patterns, pronounced differences among species underscore the importance of species-specific analyses. These variations are critical for understanding how individual tree species respond to environmental drivers, and for assessing the implications for herbivores that depend on

the tree species. Solar radiation emerged as a key driver of long-term young leaf phenology, shaping the overall trends observed in this study. While CO₂ fertilization likely contributed to long-term increases in productivity for some species, declines in young leaf production at the beginning (~2001) and near the end (~2019) of the study period highlight the dominant role of solar radiation in influencing phenological patterns. These findings reinforce the need to consider multiple environmental drivers and their interplay when analyzing long-term trends in tropical forests. As climate change continues to alter tropical ecosystems, integrating species-specific long-term data with community-wide trends will be essential to predict ecosystem dynamics and to inform conservation strategies for both plant and animal species.

Acknowledgments

Funding for this research was provided by the Baden-Württemberg Stiftung and the Max Planck Institute for Animal Behavior. We would like to thank the field assistants for the continuous data collection over the years.

References

- Abatzoglou, J. T., Dobrowski, S. Z., Parks, S. A., & Hegewisch, K. C. (2018). TerraClimate, a high-resolution global dataset of monthly climate and climatic water balance from 1958–2015. *Scientific Data* 2018 5:1, 5(1), 1–12. <https://doi.org/10.1038/sdata.2017.191>
- Ainsworth, E. A., & Rogers, A. (2007). The response of photosynthesis and stomatal conductance to rising [CO₂]: mechanisms and environmental interactions. *Plant, Cell & Environment*, 30(3), 258–270. <https://doi.org/10.1111/j.1365-3040.2007.01641.x>
- Barlow, J., França, F., Gardner, T. A., Hicks, C. C., Lennox, G. D., Berenguer, E., Castello, L., Economo, E. P., Ferreira, J., Guénard, B., Gontijo Leal, C., Isaac, V., Lees, A. C., Parr, C. L., Wilson, S. K., Young, P. J., & Graham, N. A. J. (2018). The future of hyperdiverse tropical ecosystems. *Nature*, 559(7715), 517–526. <https://doi.org/10.1038/s41586-018-0301-1>
- Barone, J. A. (1998). Effects of light availability and rainfall on leaf production in a moist tropical forest in central Panama. *Journal of Tropical Ecology*, 14, 309–321. <https://doi.org/10.1017/S0266467498000248>
- Beever, E. A., Hall, L. E., Varner, J., Loosen, A. E., Dunham, J. B., Gahl, M. K., Smith, F. A., & Lawler, J. J. (2017). Behavioral flexibility as a mechanism for coping with climate change. *Frontiers in Ecology and the Environment*, 15(6), 299–308. <https://doi.org/10.1002/fee.1502>
- Brando, P. M., Paolucci, L., Ummenhofer, C. C., Ordway, E. M., Hartmann, H., Cattau, M. E., Rattis, L., Medjibe, V., Coe, M. T., & Balch, J. (2019). Droughts, Wildfires, and Forest Carbon Cycling: A Pan-tropical Synthesis. *Annual Review of Earth and Planetary Sciences*, 47(1), 555–581. <https://doi.org/10.1146/annurev-earth-082517-010235>
- Bürkner, P.-C. (2017). **brms**: An R Package for Bayesian Multilevel Models Using Stan. *Journal of Statistical Software*, 80(1), 1–28. <https://doi.org/10.18637/jss.v080.i01>
- Campos, F. A. (2018). *A Synthesis of Long-Term Environmental Change in Santa Rosa, Costa Rica* (pp. 331–358). https://doi.org/10.1007/978-3-319-98285-4_16
- Chang-Yang, C., Sun, I., Tsai, C., Lu, C., & Hsieh, C. (2016). ENSO and frost codetermine decade-long temporal variation in flower and seed production in a subtropical rain forest. *Journal of Ecology*, 104(1), 44–54. <https://doi.org/10.1111/1365-2745.12481>

- Chapman, C. A., & Chapman, L. J. (1997). Forest Regeneration in Logged and Unlogged Forests of Kibale National Park, Uganda. *Biotropica*, 29(4), 396–412. <https://doi.org/10.1111/j.1744-7429.1997.tb00035.x>
- Chapman, C. A., & Chapman, L. J. (1999). Implications of small scale variation in ecological conditions for the diet and density of red colobus monkeys. *Primates*, 40(1), 215–231. <https://doi.org/10.1007/BF02557712/METRICS>
- Chapman, C. A., & Chapman, L. J. (2002). Foraging challenges of red colobus monkeys: influence of nutrients and secondary compounds. *Comparative Biochemistry and Physiology Part A: Molecular & Integrative Physiology*, 133(3), 861–875. [https://doi.org/10.1016/S1095-6433\(02\)00209-X](https://doi.org/10.1016/S1095-6433(02)00209-X)
- Chapman, C. A., Chapman, L. J., Jacob, A. L., Rothman, J. M., Omeja, P., Reyna-Hurtado, R., Hartter, J., & Lawes, M. J. (2010). Tropical tree community shifts: Implications for wildlife conservation. *Biological Conservation*, 143(2), 366–374. <https://doi.org/10.1016/j.biocon.2009.10.023>
- Chapman, C. A., Galán-Acedo, C., Gogarten, J. F., Hou, R., Lawes, M. J., Omeja, P. A., Sarkar, D., Sugiyama, A., & Kalbitzer, U. (2021). A 40-year evaluation of drivers of African rainforest change. *Forest Ecosystems*, 8(1). <https://doi.org/10.1186/s40663-021-00343-7>
- Chapman, C. A., Gogarten, J. F., Golooba, M., Urs Kalbitzer, |, Patrick, |, Omeja, A., Opito, E. A., & Dipto Sarkar, |. (2023). Fifty+ years of primate research illustrates complex drivers of abundance and increasing primate numbers. *Wiley Online LibraryCA Chapman, JF Gogarten, M Golooba, U Kalbitzer, PA Omeja, EA Opito, D SarkarAmerican Journal of Primatology, 2023•Wiley Online Library*. <https://doi.org/10.1002/ajp.23577>
- Chapman, C. A., & Lambert, J. E. (2000). Habitat alteration and the conservation of African primates: Case study of Kibale National Park, Uganda. *American Journal of Primatology*, 50(3), 169–185. [https://doi.org/10.1002/\(SICI\)1098-2345\(200003\)50:3<169::AID-AJP1>3.0.CO;2-P](https://doi.org/10.1002/(SICI)1098-2345(200003)50:3<169::AID-AJP1>3.0.CO;2-P)
- Chapman, C. A., Valenta, K., Bonnell, T. R., Brown, K. A., & Chapman, L. J. (2018). Solar radiation and ENSO predict fruiting phenology patterns in a 15-year record from Kibale National Park, Uganda. *Biotropica*, 50(3), 384–395. <https://doi.org/10.1111/btp.12559>
- Chen, X., Ciais, P., Maignan, F., Zhang, Y., Bastos, A., Liu, L., Bacour, C., Fan, L., Gentine, P., Goll, D., Green, J., Kim, H., Li, L., Liu, Y., Peng, S., Tang, H., Viovy, N., Wigneron, J. P., Wu, J., ... Zhang, H. (2021). Vapor Pressure Deficit and Sunlight Explain Seasonality of Leaf Phenology and Photosynthesis Across Amazonian Evergreen Broadleaved Forest. *Global Biogeochemical Cycles*, 35(6). <https://doi.org/10.1029/2020GB006893>
- Didan, K. (2021a). *MODIS/Aqua Vegetation Indices 16-Day L3 Global 250m SIN Grid V061 [Data set]*. NASA EOSDIS Land Processes Distributed Active Archive Center. Accessed 2024-11-18 from <https://doi.org/10.5067/MODIS/MYD13Q1.061>.
- Didan, K. (2021b). *MODIS/Terra Vegetation Indices 16-Day L3 Global 250m SIN Grid V061 [Data set]*. NASA EOSDIS Land Processes Distributed Active Archive Center. Accessed 2024-11-18 from <https://doi.org/10.5067/MODIS/MOD13Q1.061>.
- Didan, K., Barreto Munoz, A., Solano, R., & Huete, A. (2015). MODIS Vegetation Index User's Guide (MOD13 Series). *University of Arizona: Vegetation Index and Phenology Lab*. <http://vip.arizona.edu>
- du Plessis, K. L., Martin, R. O., Hockey, P. A. R., Cunningham, S. J., & Ridley, A. R. (2012). The costs of keeping cool in a warming world: implications of high temperatures for foraging,

- thermoregulation and body condition of an arid-zone bird. *Global Change Biology*, 18(10), 3063–3070. <https://doi.org/10.1111/J.1365-2486.2012.02778.X>
- Gabry, J., Češnovar, R., Johnson, A., & Bronder, S. (2024). *cmdstanr: R Interface to “CmdStan”* (0.7.1). <https://discourse.mc-stan.org>. <https://mc-stan.org/cmdstanr/>
- Gao, X., Huete, A. R., Ni, W., & Miura, T. (2000). Optical–Biophysical Relationships of Vegetation Spectra without Background Contamination. *Remote Sensing of Environment*, 74(3), 609–620. [https://doi.org/10.1016/S0034-4257\(00\)00150-4](https://doi.org/10.1016/S0034-4257(00)00150-4)
- Gonçalves, N. B., Lopes, A. P., Dalagnol, R., Wu, J., Pinho, D. M., & Nelson, B. W. (2020). Both near-surface and satellite remote sensing confirm drought legacy effect on tropical forest leaf phenology after 2015/2016 ENSO drought. *Remote Sensing of Environment*, 237. <https://doi.org/10.1016/j.rse.2019.111489>
- Gorelick, N., Hancher, M., Dixon, M., Ilyushchenko, S., Thau, D., & Moore, R. (2017). Google Earth Engine: Planetary-scale geospatial analysis for everyone. *Remote Sensing of Environment*, 202, 18–27. <https://doi.org/10.1016/J.RSE.2017.06.031>
- Graham, T. L., Matthews, H. D., & Turner, S. E. (2016). A Global-Scale Evaluation of Primate Exposure and Vulnerability to Climate Change. *International Journal of Primatology*, 37(2), 158–174. <https://doi.org/10.1007/s10764-016-9890-4>
- Harris, I., Osborn, T. J., Jones, P., & Lister, D. (2020). Version 4 of the CRU TS monthly high-resolution gridded multivariate climate dataset. *Scientific Data*, 7(1), 109. <https://doi.org/10.1038/s41597-020-0453-3>
- Hastenrath, S. (1985). *Climate and circulation of the tropics* (Vol. 8). Springer Netherlands. <https://doi.org/10.1007/978-94-009-5388-8>
- Hawes, J. E., & Peres, C. A. (2014). Ecological correlates of trophic status and frugivory in neotropical primates. *Oikos*, 123(3), 365–377. <https://doi.org/10.1111/j.1600-0706.2013.00745.x>
- Huete, A. R., Didan, K., Miura, T., Rodriguez, E. P., Gao, X., & Ferreira, L. G. (2002). Overview of the radiometric and biophysical performance of the MODIS vegetation indices. *Remote Sensing of Environment*, 83(1–2), 195–213. [https://doi.org/10.1016/S0034-4257\(02\)00096-2](https://doi.org/10.1016/S0034-4257(02)00096-2)
- Huete, A. R., Didan, K., Shimabukuro, Y. E., Ferreira, L. G., & Rodriguez, E. (2000). Regional Amazon basin and global analyses of MODIS vegetation indices: early results and comparisons with AVHRR. *IGARSS 2000. IEEE 2000 International Geoscience and Remote Sensing Symposium. Taking the Pulse of the Planet: The Role of Remote Sensing in Managing the Environment. Proceedings (Cat. No.00CH37120)*, 2, 536–538. <https://doi.org/10.1109/IGARSS.2000.861621>
- Huete, A. R., Didan, K., Shimabukuro, Y. E., Ratana, P., Saleska, S. R., Hutyrá, L. R., Yang, W., Nemani, R. R., & Myneni, R. (2006). Amazon rainforests green-up with sunlight in dry season. *Geophysical Research Letters*, 33(6). <https://doi.org/10.1029/2005GL025583>
- IPCC. (2022). *Climate Change 2022 – Impacts, Adaptation and Vulnerability: Working Group II Contribution to the Sixth Assessment Report of the Intergovernmental Panel on Climate Change*. Cambridge University Press. <https://doi.org/10.1017/9781009325844>
- IUCN. *IUCN Spatial Data*. (2018). <http://www.iucnredlist.org/Technical-Documents/Spatial-Data>.
- Janssen, T., Van Der Velde, Y., Hofhansl, F., Luysaert, S., Naudts, K., Driessen, B., Fleischer, K., & Dolman, H. (2021). Drought effects on leaf fall, leaf flushing and stem growth in the Amazon forest:

Reconciling remote sensing data and field observations. *Biogeosciences*, 18(14), 4445–4472. <https://doi.org/10.5194/BG-18-4445-2021>

- Karlsson, K.-G., Riihelä, A., Trentmann, J., Stengel, M., Solodovnik, I., Meirink, J. F., Devasthale, A., Jämskeläinen, E., Kallio-Myers, V., Eliasson, S., Benas, N., Johansson, E., Stein, D., Finkensieper, S., Håkansson, N., Akkermans, T., Clerbaux, N., Selbach, N., Marc, S., & Hollmann, R. (2023). *CLARA-A3: CM SAF cLOUD, Albedo and surface RAdiation dataset from AVHRR data - Edition 3*. Satellite Application Facility on Climate Monitoring (CM SAF). https://doi.org/10.5676/EUM_SAF_CM/CLARA_AVHRR/V003
- Keenan, T. F., Hollinger, D. Y., Bohrer, G., Dragoni, D., Munger, J. W., Schmid, H. P., & Richardson, A. D. (2013). Increase in forest water-use efficiency as atmospheric carbon dioxide concentrations rise. *Nature*, 499(7458), 324–327. <https://doi.org/10.1038/nature12291>
- Khaliq, I., Hof, C., Prinzing, R., Böhning-Gaese, K., & Pfenninger, M. (2014). Global variation in thermal tolerances and vulnerability of endotherms to climate change. *Proceedings of the Royal Society B: Biological Sciences*, 281(1789). <https://doi.org/10.1098/rspb.2014.1097>
- Kobayashi, S., Ota, Y., Harada, Y., Ebata, A., Moriwa, M., Onoda, H., Onogi, K., Kamahori, H., Kobayashi, C., Endo, H., Miyaoka, K., & Kiyotoshi, T. (2015). The JRA-55 reanalysis: General specifications and basic characteristics. *Journal of the Meteorological Society of Japan*, 93(1), 5–48. <https://doi.org/10.2151/jmsj.2015-001>
- Lan, X., Trans, P., & Thoning, K. W. (2024, July). *Trends in globally-averaged CO2 determined from NOAA Global Monitoring Laboratory measurements. Version 2024-07*. <https://doi.org/10.15138/9NOH-ZH07>
- Lauer, P., Chapman, C. A., Omeja, P., Rothman, J. M., & Kalbitzer, U. (n.d.). A long-term study on food choices and nutritional goals of a leaf-eating primate. *Ecosphere*.
- Lewis, S. L., Malhi, Y., & Phillips, O. L. (2004). Fingerprinting the impacts of global change on tropical forests. *Philosophical Transactions of the Royal Society B: Biological Sciences*, 359(1443), 437–462. <https://doi.org/10.1098/rstb.2003.1432>
- Linder, J. M., Cronin, D. T., Ting, N., Abwe, E. E., Davenport, T., Detwiler, K. M., Galat, G., Galat-Luong, A., Hart, J. A., Ikema, R. A., Kivai, S. M., Koné, I., Kujirakwinja, D., Maisels, F., Oates, J. F., & Struhaker, T. T. (2021). Red colobus (*Ptilocolobus*) conservation action plan 2021-2026. In *Red colobus (Ptilocolobus) conservation action plan 2021-2026*. IUCN, International Union for Conservation of Nature. <https://doi.org/10.2305/IUCN.CH.2021.08.EN>
- Liu, L., Ciais, P., Maignan, F., Zhang, Y., Viovy, N., Peaucelle, M., Kearsley, E., Hufkens, K., Bauters, M., Chapman, C. A., Fu, Z., Lin, S., Lu, H., Ren, J., Yang, X., He, X., & Chen, X. (2024). Solar Radiation Triggers the Bimodal Leaf Phenology of Central African Evergreen Broadleaved Forests. *Journal of Advances in Modeling Earth Systems*, 16(7), 1–21. <https://doi.org/10.1029/2023MS004014>
- Lloyd, J., & Farquhar, G. D. (2008). Effects of rising temperatures and [CO₂] on the physiology of tropical forest trees. *Philosophical Transactions of the Royal Society B: Biological Sciences*, 363(1498), 1811–1817. <https://doi.org/10.1098/rstb.2007.0032>
- Mahlstein, I., Knutti, R., Solomon, S., & Portmann, R. W. (2011). Early onset of significant local warming in low latitude countries. *Environmental Research Letters*, 6(3). <https://doi.org/10.1088/1748-9326/6/3/034009>

- Malhi, Y., Gardner, T. A., Goldsmith, G. R., Silman, M. R., & Zelazowski, P. (2014). Tropical forests in the anthropocene. In *Annual Review of Environment and Resources* (Vol. 39, pp. 125–159). Annual Reviews Inc. <https://doi.org/10.1146/annurev-enviro-030713-155141>
- Marchant, R., Mumbi, C., Behera, S., & Yamagata, T. (2007). The Indian Ocean dipole - The unsung driver of climatic variability in East Africa. In *African Journal of Ecology* (Vol. 45, Issue 1, pp. 4–16). <https://doi.org/10.1111/j.1365-2028.2006.00707.x>
- Matsuda, I., Ihobe, H., Tashiro, Y., Yumoto, T., Baranga, D., & Hashimoto, C. (2020). The diet and feeding behavior of the black-and-white colobus (*Colobus guereza*) in the Kalinzu Forest, Uganda. *Primates*, 61(3), 473–484. <https://doi.org/10.1007/s10329-020-00794-6>
- McFarland, R., Barrett, L., Boner, R., Freeman, N. J., & Henzi, S. P. (2014). Behavioral flexibility of vervet monkeys in response to climatic and social variability. *American Journal of Physical Anthropology*, 154(3), 357–364. <https://doi.org/10.1002/ajpa.22518>
- Ozgul, A., Fichtel, C., Paniw, M., & Kappeler, P. M. (2023). Destabilizing effect of climate change on the persistence of a short-lived primate. *Proceedings of the National Academy of Sciences of the United States of America*, 120(14). <https://doi.org/10.1073/pnas.2214244120>
- Paniw, M., Maag, N., Cozzi, G., Clutton-Brock, T., & Ozgul, A. (2019). Life history responses of meerkats to seasonal changes in extreme environments. In *Science* (Vol. 363, Issue 6427, pp. 631–635). American Association for the Advancement of Science. <https://doi.org/10.1126/science.aau5905>
- Pedersen, E. J., Miller, D. L., Simpson, G. L., & Ross, N. (2019). Hierarchical generalized additive models in ecology: an introduction with mgcv. *PeerJ*, 7, e6876. <https://doi.org/10.7717/peerj.6876>
- Piao, S., Wang, X., Park, T., Chen, C., Lian, X., He, Y., Bjerke, J. W., Chen, A., Ciais, P., Tømmervik, H., Nemani, R. R., & Myneni, R. B. (2019). Characteristics, drivers and feedbacks of global greening. *Nature Reviews Earth & Environment*, 1(1), 14–27. <https://doi.org/10.1038/s43017-019-0001-x>
- R Core Team. (2023). *R: A Language and Environment for Statistical Computing* (4.3.2). R Foundation for Statistical Computing. <https://www.R-project.org/>
- Saji, N., & Yamagata, T. (2003). Possible impacts of Indian Ocean Dipole mode events on global climate. *Climate Research*, 25, 151–169. <https://doi.org/10.3354/cr025151>
- Skorupa, J. P. (1988). *The effects of selective timber harvesting on rain-forest primates in Kibale Forest, Uganda* [University of California, Davis]. <https://search.proquest.com/openview/b420199aed4550fc2d2770566b7c9062/1?pq-origsite=gscholar&cbl=18750&diss=y>
- Struhsaker, T. T. (1975). *The Red Colobus Monkey*. University of Chicago Press, Chicago. https://scholar.google.com/scholar?hl=de&as_sdt=0%2C5&q=The+Red+Colobus+Monkey%2C++Chicago+%281975%29+struhsaker&btnG=
- Struhsaker, T. T. (1997). Ecology of an African rain forest: logging in Kibale and the conflict between conservation and exploitation. University of Florida Press, Gainesville. <https://www.cabidigitallibrary.org/doi/full/10.5555/20000617542>
- Sullivan, M. K., Fayolle, A., Bush, E., Ofosu-Bamfo, B., Vleminckx, J., Metz, M. R., & Queenborough, S. A. (2024). Cascading effects of climate change: new advances in drivers and shifts of tropical reproductive phenology. *Plant Ecology*, 225(3), 175–187. <https://doi.org/10.1007/s11258-023-01377-3>

- Timmermann, A., An, S. Il, Kug, J. S., Jin, F. F., Cai, W., Capotondi, A., Cobb, K., Lengaigne, M., McPhaden, M. J., Stuecker, M. F., Stein, K., Wittenberg, A. T., Yun, K. S., Bayr, T., Chen, H. C., Chikamoto, Y., Dewitte, B., Dommenges, D., Grothe, P., ... Zhang, X. (2018). El Niño–Southern Oscillation complexity. In *Nature* (Vol. 559, Issue 7715, pp. 535–545). Nature Publishing Group. <https://doi.org/10.1038/s41586-018-0252-6>
- van Schaik, C. P., & Pfannes, K. R. (2005). Tropical climates and phenology: a primate perspective. *Cambridge Studies in Biological and Evolutionary Anthropology*, 44, 23. <https://www.cambridge.org/core/services/aop-cambridge-core/content/view/4BBF738CCE9C4B8A83A74493A4A632B3>
- Van Schaik, C. P., Terborgh, J. W., & Wright, S. J. (1993). *The Phenology of Tropical Forests: Adaptive Significance and Consequences for Primary Consumers* (Vol. 24). <https://about.jstor.org/terms>
- Vehtari, A., Gelman, A., & Gabry, J. (2017). Practical Bayesian model evaluation using leave-one-out cross-validation and WAIC. *Statistics and Computing*, 27(5), 1413–1432. <https://doi.org/10.1007/s11222-016-9696-4>
- Wagner, F. H., Hérault, B., Rossi, V., Hilker, T., Maeda, E. E., Sanchez, A., Lyapustin, A. I., Galvão, L. S., Wang, Y., & Aragão, L. E. O. C. (2017). Climate drivers of the Amazon forest greening. *PLoS ONE*, 12(7). <https://doi.org/10.1371/journal.pone.0180932>
- Wang, S., Zhang, Y., Ju, W., Chen, J. M., Ciais, P., Cescatti, A., Sardans, J., Janssens, I. A., Wu, M., Berry, J. A., Campbell, E., Fernández-Martínez, M., Alkama, R., Sitch, S., Friedlingstein, P., Smith, W. K., Yuan, W., He, W., Lombardozi, D., ... Peñuelas, J. (2020). Recent global decline of CO₂ fertilization effects on vegetation photosynthesis. *Science*, 370(6522), 1295–1300. <https://doi.org/10.1126/science.abb7772>
- Waterman, P. G., & Kool, K. M. (1994). Colobine food selection and plant chemistry. In *Colobine monkeys: Their ecology, behaviour and evolution*.
- Williams, J. W., Jackson, S. T., & Kutzbach, J. E. (2007). Projected distributions of novel and disappearing climates by 2100 AD. *Proceedings of the National Academy of Sciences*, 104(14), 5738–5742. <https://doi.org/10.1073/pnas.0606292104>
- Wright, S. J., & van Schaik, C. P. (1994). Light and the Phenology of Tropical Trees. *American Naturalist*, 143(1), 192–199.
- Xiao, X., Braswell, B., Zhang, Q., Boles, S., Frohling, S., & Moore, B. (2003). Sensitivity of vegetation indices to atmospheric aerosols: continental-scale observations in Northern Asia. *Remote Sensing of Environment*, 84(3), 385–392. [https://doi.org/10.1016/S0034-4257\(02\)00129-3](https://doi.org/10.1016/S0034-4257(02)00129-3)
- Yang, X., Wu, J., Chen, X., Ciais, P., Maignan, F., Yuan, W., Piao, S., Yang, S., Gong, F., Su, Y., Dai, Y., Liu, L., Zhang, H., Bonal, D., Liu, H., Chen, G., Lu, H., Wu, S., Fan, L., ... Wright, S. J. (2021). A comprehensive framework for seasonal controls of leaf abscission and productivity in evergreen broad-leaved tropical and subtropical forests. *Innovation*, 2(4). <https://doi.org/10.1016/j.xinn.2021.100154>
- Zelazowski, P., Malhi, Y., Huntingford, C., Sitch, S., & Fisher, J. B. (2011). Changes in the potential distribution of humid tropical forests on a warmer planet. *Philosophical Transactions of the Royal Society A: Mathematical, Physical and Engineering Sciences*, 369(1934), 137–160. <https://doi.org/10.1098/rsta.2010.0238>

Zhang, J., Li, Y., Yang, Y., Garber, P. A., Han, K., Huang, Z., Cui, L., & Xiao, W. (2023). Effects of food availability and climate on the activity budget of Shortridge's langur (*Trachypithecus shortridgei*) in the Drung Valley, Gaoligong Mountains, China. *American Journal of Primatology*. <https://doi.org/10.1002/ajp.23467>

Zhu, Z., Piao, S., Myneni, R. B., Huang, M., Canadell, J. G., Ciais, P., Sitch, S., Friedlingstein, P., Arneeth, A., Cao, C., Cheng, L., Kato, E., Koven, C., Lian, X., Liu, Y., Liu, R., Mao, J., Pan, Y., Peñuelas, J., ... Zeng, N. (2016). Greening of the Earth and its drivers. *Nature.Com*. <https://doi.org/10.1038/NCLIMATE3004>

Supplementary Information

EVI

We extracted EVI values for our study area for the period between February 2000 and December 2021 using the Terra-MODIS 250m 16-day V6.1 product MOD13Q1 (Feb 2000 – Dec 2021; Didan, 2021b) and the Aqua-MODIS 250m 16-day V6.1 product MY13Q1 V6.1 (Jul 2002 – Dec 2021; Didan, 2021a) accessed via Google Earth Engine (Didan et al., 2015; Gorelick et al., 2017). The study area was defined by a polygon with the following coordinates: (30.3489°E, 0.5014°N), (30.3595°E, 0.4252°N), (30.4749°E, 0.4369°N), (30.4968°E, 0.5344°N), (30.4323°E, 0.6188°N), (30.3650°E, 0.6065°N), (30.3513°E, 0.5866°N), and (30.3547°E, 0.5639°N), returning to the starting point at (30.3489°E, 0.5014°N). These coordinates define the boundaries of the polygon, representing the study area in the northern region of Kibale. To ensure high data quality, we applied filtering based on the MODIS SummaryQA band, retaining only pixels flagged as "good quality," while masking out those affected by cloud cover, shadows, or atmospheric distortions (Didan et al., 2015). By combining the Terra and Aqua data streams, we produced a quasi-8-day EVI time series, which enhanced our ability to detect temporal changes in vegetation dynamics and ensured sufficient data coverage even in tropical regions where persistent cloud cover is common.

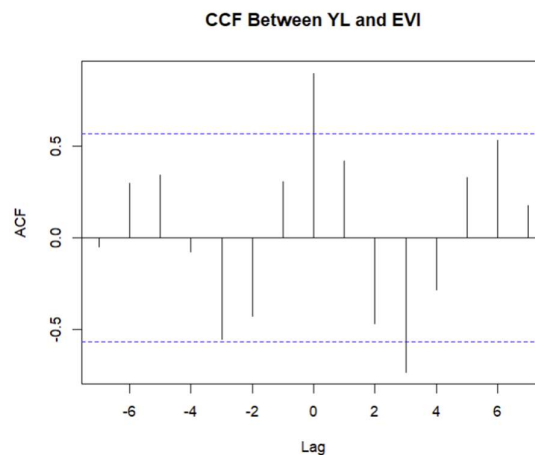


Figure S1 Time series autocorrelation function of EVI and Young leaf scores. Each monthly value is compared with each other, and also with timelags. The value 0 corresponds to no timelag, and the blue horizontal lines represent the approximate 95% confidence interval.

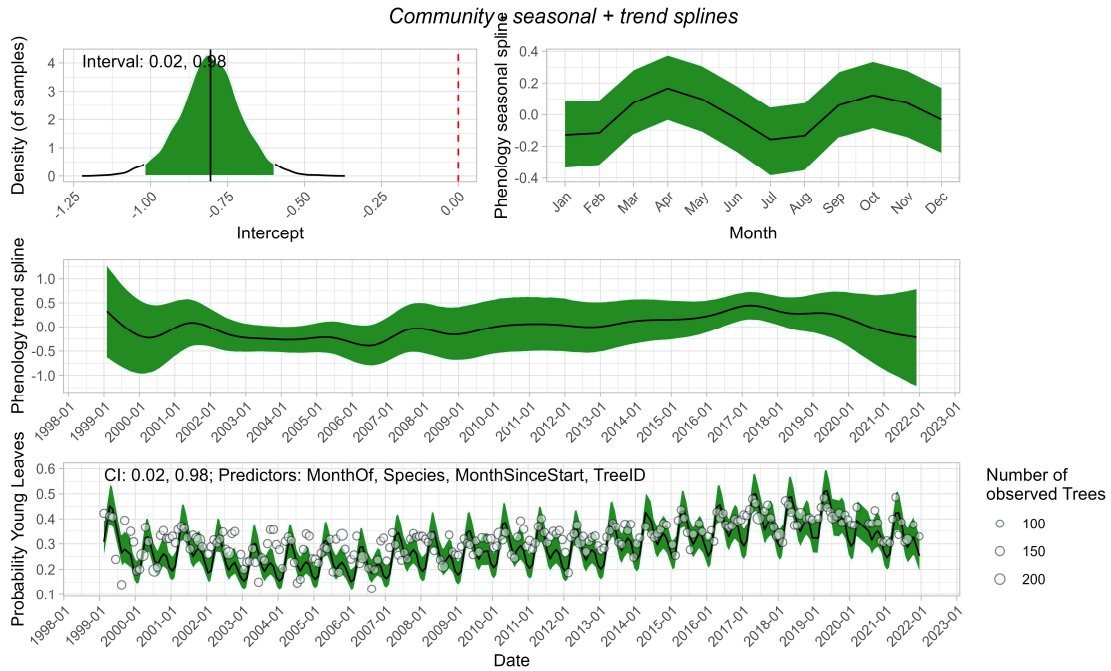


Figure S2 Community-level young leaf phenology model including data from all 12 tree species. The panels show the (a) intercept, (b) Seasonal component with Month as variable for the spline term, (c) Trend spline with month since first observation as variable for the spline term and (d) Resulting predictions of the model. Shaded areas represent the 95% credible interval of the estimated mean. Points in panel (d) represent monthly observed data, with point size scaled to the number of trees observed.

Table S1 Seasonality of species and effects of climate predictors. The last column indicates the climate predictor (and the respective timelag) included in the top model for each species, and whether it was a positive (+) or negative (-) relationship with young leaf production.

Species	Seasonal Pattern	1 st Peak	2 nd Peak	1 st Valley	2 nd Valley	Climate predictor
Community	Seasonal with two similar peaks	Apr	Oct	Feb	Jul/Aug	-
<i>Celtis gomphophylla</i> <i>Albizia grandibracteata</i>	Seasonal with higher first peak	Apr/May	Oct	Jan	Aug-	T_{max} (+) 3m <i>C.g.</i> , 6m <i>A.g.</i>
<i>Millettia dura</i> <i>Dombeya kirkii</i>	Seasonal with two similar peaks	Apr	Oct	Feb	Jul/Aug	Rainfall (+) <i>M.d.</i> Cloud cover (+) 1m <i>D.k.</i>
<i>Celtis africana</i> <i>Macaranga schweinfurthii</i> <i>Vepris nobilis</i>	Weakly seasonal with peaks during rain seasons	Apr/May	Oct/Nov	Feb	Jul/Aug	Rainfall (+) <i>C.a.</i> , 1m <i>V.n.</i> Cloud cover (+) 3m <i>M.s.</i>
<i>Prunus Africana</i> <i>Funtumia africana</i> <i>Parinari excelsa</i>	Weakly seasonal with peaks before rain seasons	Feb/Mar	Sep/Oct	Dec	May/Jun	T_{min} (-) 1m <i>P.a.</i> T_{max} (+) 1m <i>F.a.</i> Cloud cover (-) 3m <i>P.e.</i>
<i>Trilepisium madagascariense</i>	Very weakly seasonal	Mar	Nov	Dec	Jul/Aug	CO₂ (-) 6m
<i>Strombosia scheffleri</i>	Non-seasonal	-	-	-	-	Not clear

Table S2 Long-term trends of species and climatic predictors. The last column indicates the climate predictor (and the respective timelag) included in the top model for each species, and whether it was a positive (+) or negative (-) relationship with young leaf production.

<i>Species</i>	<i>Overall trend</i>	<i>Long-term pattern</i>	<i>Peaks</i>	<i>Climate Predictor</i>
<i>Community</i>	S-shape with low in 2007 and peak in 2017	Peak in 2001, drop until 2006, increase until 2017, decrease until end of study	2001, 2008, 2017	-
<i>Funtumia africana</i>	S-shape with low in 2005/06 and peak in 2018/19	Decrease until 2006, increase until 2018, decreasing from 2019 onwards.	2001, 2008, 2011, 2018	Solar radiation (+) 6m
<i>Albizia grandibracteata</i>		Decrease until 2005, increase until 2019, decrease from 2019 onwards.	2001, 2004, 2007, 2010, 2014, 2019	
<i>Trilepisium madagascariense</i>	Peak in 2001 and 2018/19, Low in 2009	Peak in 2001, decrease until 2009, increase until 2019	2001, 2011, 2019	
<i>Prunus africana</i>		Peak in 2001, decrease until 2009, increase until 2019	2001, 2008, 2019	
<i>Millettia dura</i>	Variable	Peaks in 2001, 2010 and 2018, decrease until end	2001, 2010, 2018	
<i>Vepris nobilis</i>	Increase with low in 2004	Increasing with major peaks in 2001, 2017, then decrease until 2022	2001, 2008, 2013, 2017	CO₂ (+) 1m, 3m, 6m (all timelags very close in all species)
<i>Parinari excelsa</i>		Steady increase until 2019 with major peak in 2001 and 2019, low in 2004	2001, 2008, 2019	
<i>Dombeya kirkii</i>	Increase with low in 2006	Increase with major peaks in 2001, low in 2006, increase until 2019, decrease until 2022	2001, 2010, 2019	
<i>Strombosia schaffleri</i>		S-shape with low in 2006, then steady increase until 2019	2000, 2011, 2019	
<i>Celtis africana</i>	Steady increase	Steady increase until 2019, slight low in 2004	2019	CO₂ (+)
<i>Celtis gomphophylla</i>	Variable	Very variable, tendency increasing	2001, 2004, 2009, 2011, 2015, 2017, 2019, 2022	Cloud cover (+) 1m
<i>Macaranga schweinfurthii</i>	Variable	Variable, except for drop in 2014 and end of study due to no data (trees dying)	2017	Solar radiation (-) 1m